$$\frac{1}{2}(I_s^2 + I_d^2) \simeq 1/c_0 \int_0^{c_0} D(c)dc \qquad (3.7)$$

Other methods such as use of successively smaller intervals and weighted mean diffusion coefficients for systems such as this are fully discussed in ref 3 and 4.

Diffusion in samples of different geometry require solutions of the equation

$$\frac{\partial c}{\partial t} = \text{div}\{D(c) \text{ grad } c\} \qquad (3.8)$$

Swelling effects can be minimized by employing a section fixed frame of reference. It is desirable to have both sorption and permeation measurements on such a system to verify the basic equilibrium assumption of the theory. Agreement must exist between values of $D(c)$ obtained from transient and steady-state measurements. The theory has been developed for homogeneous polymer-gas systems that are studied sufficiently well above their glass transition temperatures so that non-Fickian transport effects could be neglected.

Acknowledgments. We are indebted to Dr. R. Eby for drawing our attention to this problem and we acknowledge helpful discussions with Drs. G. T. Davis and R. Eby. Acknowledgment is made to the donors of the Petroleum Research Fund, administered by the American Chemical Society, for partial support of this work and to the National Science Foundation (NSF Grant R019881001).

Aspects of Polymer–Polymer Thermodynamics

Lee P. McMaster

Union Carbide Corporation, Bound Brook, New Jersey. *Received March 6, 1973*

ABSTRACT: It has been observed that most polymer–polymer pairs exhibiting partial miscibility decrease in solubility as temperature is increased. One origin of the observed behavior has been found to arise from free volume effects. Using a modified form of Flory's "equation of state" thermodynamics, it has been shown that lower critical solution temperature (lcst) behavior should generally be anticipated for polymer–polymer systems. Rather modest differerences in pure-component thermal expansion coefficients are responsible for the lcst. Computations have been made which show the effect of molecular weight, pure-component equation of state parameters, the interaction energy parameter, and other mixture parameters on polymer–polymer mutual solubility. In addition, the effects of pressure and polydispersity have been considered. The cloud point curves for two polymer–polymer pairs have been measured; comparison of these curves with the theoretical curves show them to have less temperature sensitivity. Reasons for this quantitative discrepancy are discussed.

During the last few years considerable effort has been expended by the polymer industry to identify compatible polymer pairs. The reason for the effort is that thermodynamic solubility of one polymer in another is the exception rather than the rule. Hence, if such systems can be found, the probability of obtaining a proprietary compatible material is high. For the same reason, research aimed at finding mutually soluble polymer pairs can be futile since the probability of success is often small. Techniques have been developed based upon use of the multidimensional solubility parameter[1-5] to aid in finding compatible polymer pairs. These procedures, although helpful, have not been entirely successful when applied to polymer–polymer systems.

In the course of research at this laboratory, it has been observed that several polymer liquids which are mutually soluble at a low temperature exhibit a liquid–liquid phase transition at higher temperatures. This lower critical solution temperature (lcst) behavior has been observed rather than the more conventional upper critical solution temperature (ucst) behavior. The purpose of this paper is to explain this rather unusual thermodynamic behavior using Flory's new "equation of state" thermodynamics.[6,7]

The model predicts why most polymer pairs show a decrease in mutual solubility as temperature is increased. This trend is contrary to predictions of the original Flory–Huggins model[8] of polymer solution thermodynamics. It is also contrary to the behavior of most polymer–solvent systems far below the critical point of the solvent. The model also predicts the qualitative effects of pressure and molecular weight distribution on the polymer thermodynamics.

An additional need for such a thermodynamic model arises when one is concerned with phase transition phenomena in binary and multicomponent polymer systems. Predictions of the mode of phase separation and the ultimate structure require a detailed thermodynamic model.

Cloud point curves have been measured experimentally for two polymer pairs. These data are used to make a qualitative comparison with the model. However, no attempt is made to determine model parameters for either experimental system.

Theoretical Development

A. The Flory "Equation of State" Thermodynamic Model. In this section, a generalized version of Flory's equation of state thermodynamics will be presented. Both similarities to and differences from the original Flory–Huggins theory of polymer solution thermodynamics will be indicated. The intention of this comparison is to provide a basis of presentation which is familiar to most polymer scientists. Of course, much of the phenomena discussed below can also be quantitatively described by the use of the Flory–Huggins theory with an empirical concentration and temperature-dependent interaction parameter. However, such empiricism provides little understanding of the underlying causes of observed thermody-

(1) P. A. Small, *J. Appl. Chem.*, **3**, 71 (1953).
(2) J. L. Gardon, *J. Paint Technol.*, **38**, 43 (1966).
(3) R. F. Blanks and J. M. Prausnitz, *Ind. Eng. Chem., Fundam.*, **3**, 1 (1964).
(4) C. M. Hansen, *J. Paint Technol.*, **39**, 104 (1967).
(5) J. D. Crowley, G. S. Teaque, Jr., and J. W. Lowe, Jr., *J. Paint Technol.*, **38**, 269 (1966).
(6) P. J. Flory, R. A. Orwoll, and A. Vrij, *J. Amer. Chem. Soc.*, **86**, 3515 (1964).
(7) P. J. Flory, *J. Amer. Chem. Soc.*, **87**, 1833 (1965).
(8) P. J. Flory, "Principles of Polymer Chemistry," Cornell University Press, Ithaca, N. Y., 1953.

namic behavior. The equation of state theory, on the other hand, provides one fundamental explanation for the generally observed lcst behavior of polymer-polymer systems. The new theory can easily be adapted so that equilibrium phase boundaries of binary polymer-polymer solutions can be computed. Thus, it is the goal of the theoretical development to derive a generalized equation for the chemical potential of a polymeric component in a binary solution. In addition, equations for the spinodal curve and the critical point will be presented. By using the results of Koningsveld *et al.*,[9] extensions to binary solutions of polydisperse polymers are also possible.

The early theories of polymer solution thermodynamics consider only two aspects of liquid mixtures. The first of these is the famous Flory-Huggins combinatorial entropy of mixing

$$\Delta S_c^m = -k\sum_{i=1}^{n} N_i \ln v_i \tag{1}$$

This entropy arises from consideration of the number of ways the segments of chain molecules can be placed into a lattice. The second aspect considers the energy interactions between neighboring segments of different types. In this regard, the early theories rely on the regular solution theory assumption of zero volume change on mixing and an internal energy of mixing given by the Scatchard-Hildebrand formula

$$\Delta E^m = \sum_{j=2}^{n}\sum_{i=1}^{j-1} N_i v_j X_{ij} \tag{2}$$

In the ideal case of pure dispersive interactions, the interaction parameter is given by

$$X_{ij} = \frac{V_i(\delta_i - \delta_j)^2}{RT} \tag{3}$$

where the δ's are the respective component solubility parameters. In most practical cases, this interaction parameter must be taken concentration dependent to account for observed behavior.

More recently, Flory has demonstrated that polymer solution thermodynamics also depend on the local liquid structure. These effects are generally referred to as "free volume" effects and much has been written about them in the recent literature.[7,10-14] Although not entirely successful from a quantitative point of view, Flory's new solution theory is a step in the right direction. Conceptually, the new model should also be adaptable to polymer-polymer systems.

Flory's theory is derived by considering the number of ways that particles of volume, v^*, can be placed into a configurational space whose cells each have a volume, v. The volume, v^*, is the hard core volume of a polymer segment and is always less than the volume, v, the actual molecular volume of the segment. The definition of a segment is arbitrary but can usually be thought of as a monomer unit or some multiple of a monomer unit. Hence, additional volume in phase space is accessible to the system because of the presence of the free volume. This expanded configurational space must be accounted for in the configurational integral for the system.

(9) R. Koningsveld, H. A. G. Chermin, and M. Gordon, *Proc. Roy. Soc., Ser. A*, **319**, 331 (1970).
(10) D. Patterson and G. Delmas, *Trans. Faraday Soc.*, **65**, 708 (1969).
(11) D. Patterson, G. Delmas, and T. Somcynsky, *Polymer*, **8**, 503 (1967).
(12) K. S. Siow, G. Delmas, and D. Patterson, *Macromolecules*, **5**, 29 (1972).
(13) L. Zeman, J. Biros, G. Delmas, and D. Patterson, *J. Phys. Chem.*, **76**, 1206 (1972).
(14) L. Zeman and D. Patterson, *J. Phys. Chem.*, **76**, 1214 (1972).

In addition, the lattice energy is assumed to be volume dependent of the form

$$E_i(0) \alpha 1/v^n \tag{4}$$

Based upon energy of vaporization data, n can be anticipated to be in the range[15]

$$1.0 < n < 1.5 \tag{5}$$

Flory also assumes that the intersegmental energy can be treated as arising from interactions between the surfaces of adjoining segments. Using these assumptions, he obtains the pure component equation of state by differentiating the defining equation for the pressure of the system.

$$P = \frac{kT}{N_i r_i}\left.\frac{\partial \ln Z_i}{\partial v_i}\right|_{T,N_i} \tag{6}$$

In this equation, Z_i is the partition function[16a] of the Flory theory,[7] r_i is the number of segments per molecule, N_i is the number of molecules, and k is Boltzmann's constant. The resulting equation of state is

$$\frac{\bar{P}_i \bar{v}_i}{\bar{T}_i} = \frac{\bar{v}_i^{1/3}}{\bar{v}_i^{1/3} - 1} - \frac{1}{\bar{T}_i \bar{v}_i^{n}} \tag{7}$$

where

$$\bar{P}_i = P/P_i^* \tag{8}$$

$$\bar{T}_i = T/T_i^* \tag{9}$$

$$\bar{v}_i = v_i/v^* \tag{10}$$

The starred quantities are the parameters of the equation of state. These parameters can be obtained from measurements of the thermal expansion coefficient

$$\alpha = \frac{1}{v}\left.\frac{\partial v}{\partial T}\right|_{P,N_i}$$

and the thermal pressure coefficient

$$\gamma = \left.\frac{\partial P}{\partial T}\right|_{V,N_i}$$

(15) J. H. Hildebrand, J. M. Prausnitz, and R. L. Scott, "Regular and Related Solutions," Von Nostrand-Reinhold Co., Princeton, N. J., 1970, p 61.
(16) (a) The generalized partition function assumes the form

$$Z_i(T,V) = Z_{int}(T)\left(\frac{2\pi m_i kT}{h^2}\right)^{3/2N_i r_i c_i} Q_i$$

where

$$Q_i = Q_i(\text{comb})\left[\frac{4\pi}{3}\{v_i(r_i^{1/3} - r^{*1/3})^3 N_i r_i c_i\}\right]\times \exp(-E_i(0)/kT)$$

The partition function in this form is obtained by separating the $3c_i$ external degrees of freedom from the internal degrees of freedom. The internal or intramolecular degrees of freedom constitute modes of high frequency which are essentially unaffected by neighbors in the liquid.[6] These intramolecular rotational and vibrational frequencies are functions of temperature only and, hence, do not enter into the equation of state. The external or intermolecular degrees of freedom comprise lower frequency modes in the isolated molecule. These modes are subject to weaker intramolecular potentials so that interactions with neighboring chain segments dominate. The weaker intramolecular potentials can be disregarded or treated as effective translational motions. The terms used in the partition function are defined in the text. The interested reader should see Flory[7] for the derivation of this partition function. (b) I. Prigogine, "The Molecular Theory of Solutions," North-Holland Publishing Co., Amsterdam, 1957.

Table I
Assumed Equalities for Polydisperse Polymer Pairs

Equality	Over	Parameter Description
$m_i = m_1$	$i = 1, \ldots, m$	Mass/segment
$m_i = m_2$	$i = m+1, \ldots, n$	Mass/segment
$\tilde{v}_i = \tilde{v}_1$	$i \leq m$	Reduced volume
$\tilde{v}_i = \tilde{v}_2$	$i \geq m+1$	Reduced volume
$P_i^* = P_1^*$	$i \leq m$	Pressure parameter
$P_i^* = P_2^*$	$i \geq m+1$	Pressure parameter
$T_i^* = T_1^*$	$i \leq m$	Temperature parameter
$T_i^* = T_2^*$	$i \geq m+1$	Temperature parameter
$c_{ij} = 0$	$i \leq m, j \leq m$ or $i \geq m+1$, $j \geq m+1$	Degrees of freedom
$= \tilde{c}_{12}$	$i \leq m, j \geq m+1$	Degrees of freedom
$X_{ij}' = 0$	$i \leq m, j \leq m$ or $i \geq m+1$, $j \geq m+1$	Energy interaction
$= \overline{X}_{12}$	$i \leq m, j \geq m+1$	Energy interaction
$Q_{ij} = 0$	$i \leq m, j \leq m$ or $i \geq m+1$, $j \geq m+1$	Entropy interaction
$Q_{ij} = \overline{Q}_{12}$	$i \leq m, j \geq m+1$	Entropy interaction

both extrapolated to zero pressure. The results are

$$\tilde{v}_i = \left[\frac{\alpha_i(P=0)T}{3n\alpha_i(P=0)+3} + 1\right]^3 \tag{11}$$

$$\overline{T}_i = \frac{\overline{v}_i^{1/3} - 1}{\overline{v}_i^{n+1/3}} \tag{12}$$

and

$$P_i^* = \gamma_i(P=0)T\overline{v}_i^{n+1} \tag{13}$$

A similar equation of state can be derived for a multicomponent mixture by adding at least one additional set of free parameters (X_{ij}'). These parameters arise from considering the differences in interaction energy for unlike segmental pairs. They correspond to the parameter X_{ij} (eq 2) of the Flory-Huggins theory.[16a]

Two other parameters have been added to the most generalized version of the new theory. Eichinger and Flory[17] add an entropic term to the free energy of mixing. The parameters (Q_{ij}) of this term correspond to the entropy associated with the interaction of segments similar to the interaction energy given in terms of the X_{ij}' parameters. This entropic term is empirical; the parameters, Q_{ij}, are added to quantify the magnitude of the entropic interaction. Finally, the last parameter is a "degrees of freedom" correction term. Generally, $3c_i$ is used to characterize the number of external degrees of freedom available to the segments. These external degrees of freedom are independent of intramolecular forces. They are affected by the intermolecular forces (dispersive and polar) to which the segments are subjected. Lin[18] has assumed the number of external degrees of freedom for the mixture to be quadratic in the segment fraction, *i.e.*

$$c = \sum_{i=1}^{n} \phi_i c_i - \sum_{j=2}^{n}\sum_{i=1}^{j-1} \phi_i \phi_j c_{ij} \tag{14}$$

In this equation, ϕ_i, the segment fraction is the equivalent to the volume fraction but is based upon additive properties of the hard core volume rather than the molecular volume. The c_{ij} are quadratic correction coefficients to a linear variation in the number of external degrees of freedom.

(17) B. E. Eichinger and P. J. Flory, *Trans. Faraday Soc.*, **64**, 2035, 2053, 2061, 2066 (1968).
(18) P. H. Lin, Sc.D. Thesis, Washington U., St. Louis, Mo., 1970.

In order to determine the phase boundaries of any binary or multicomponent polymer mixture, the equation for the free energy of mixing of the mixture must be obtained. The Helmholtz free energy of mixing can be evaluated in a straightforward manner using the standard equation of statistical thermodynamics

$$\Delta F^m = -kT \ln\left(\frac{Z}{\prod_{i=1}^{n} Z_i}\right) \tag{15}$$

By considering every term in the partition function simultaneously, the generalized Helmholtz free energy of mixing for a multicomponent system becomes

$$\begin{aligned}\frac{\Delta F^m}{kT} = {} & \sum_{i=1}^{n} N_i \ln \phi_i + \\ & \sum_{i=1}^{n} 3r_i N_i (c_i - c) \ln\left[(2\pi m_i kT)^{1/2}/h\right] + \\ & 3\bar{r}N_T \sum_{j=2}^{n}\sum_{i=1}^{j-1} \phi_i \phi_j c_{ij} \ln\left[(\gamma v^*)^{1/3}(\tilde{v}^{1/3} - 1)\right] + \\ & 3\sum_{i=1}^{n} r_i N_i c_i \ln\left[\frac{\tilde{v}_i^{1/3} - 1}{\tilde{v}^{1/3} - 1}\right] + \\ & \frac{\bar{r}N_T v^*}{nkT}\left[\sum_{i=1}^{n} \phi_i P_i^* \left(\frac{1}{\tilde{v}_i^n} - \frac{1}{\tilde{v}^n}\right) + \right. \\ & \left. \sum_{j=2}^{n}\sum_{i=1}^{j-1} \phi_i \theta_j \left(\frac{X_{ij}'}{\tilde{v}^n} - nT\overline{v}_i Q_{ij}\right)\right]\end{aligned} \tag{16}$$

There are several terms in this equation which have not previously been defined. The m_i represent the mass/segment for each component. γ is a geometric parameter depending upon the number of nearest neighbors surrounding a given segment. For a segmental coordination number of 8–10, a value of $\gamma = 1.3$ is appropriate.[19a] Also

$$N_T = \sum_{i=1}^{n} N_i \tag{17}$$

$$\bar{r} = \sum_{i=1}^{n} N_i r_i / N_T \tag{18}$$

$$\theta_i = \frac{s_i r_i N_i}{\bar{s}\,\bar{r} N_T} \tag{19}$$

s_i = surface area i/segment

$$\bar{s} = \sum_{i=1}^{n} s_i r_i N_i / \bar{r} N_T \tag{20}$$

The θ_i in eq 19 represents the fraction of the total segmental surface area occupied by type i molecules. These θ_i appear in eq 16 because the segmental interaction is assumed to occur only at the surfaces of the nearest neighbor segments. The surface areas/segment are currently estimated by two routes. Flory *et al.*[17,19b,20] use values obtained from known molecular geometries. In the absence of this kind of information, the only other procedure available is the group contribution technique of Bondi[21] for computing van der Waals molecular volumes. Comparison with actual polymer solution thermodynamic measurements shows that neither procedure is entirely satisfactory for estimating surface area ratios.

(19) (a) The exact numerical value of this parameter is inconsequential in that it does not cause a significant shift in the phase boundaries even for values of γ varying by more than 100%. (b) P. J. Flory and H. Höcker, *Trans. Faraday Soc.*, 67, 2258, 2275 (1968).
(20) R. A. Orwoll and P. J. Flory, *J. Amer. Chem. Soc.*, **89**, 6814, 6822 (1967).

B. Chemical Potentials for Binary Monodisperse Systems. With the defining equation for the free energy of mixing, the chemical potentials of each component can easily be evaluated so that binodal curves can be computed. The chemical potential of each component in a multicomponent mixture is given by

$$\Delta\mu_k = \frac{\partial \Delta F^m}{\partial N_k}\Big|_{\substack{T,\bar{v},N_j \\ j\neq k}} + \frac{\partial \Delta F^m}{\partial \bar{v}}\Big|_{T,N_k,N_j} \frac{\partial \bar{v}}{\partial N_k}\Big|_{\substack{T,V,N_j \\ j\neq k}} \tag{21}$$

Flory[7,17] neglects the second term in this equation since it makes a small contribution at low pressures. This term must be included at higher pressures and even at low pressures if the effect of pressure is to be predicted correctly.

Term by term differentiation of equation 16 leads to the following equations for the chemical potentials in a binary mixture,

$$\frac{\Delta\mu_1}{kT} = \ln\phi_1 + (1 - r_1/r_2)\phi_2 + 3r_1\phi_2^2(c_1 - c_2 + 2\phi_1 c_{12}) \ln\sqrt{m_1/m_2} + 3r_1\phi_2^2 c_{12} \ln\{(2\pi m_2 kT)^{1/2}/h(\gamma v^*)^{1/3}(\bar{v}^{1/3} - 1)\} + 3r_1 c_1 \ln\left[\frac{\bar{v}_1^{1/3} - 1}{\bar{v}^{1/3} - 1}\right] + \frac{r_1 v^*}{nkT}\left[P_1^*\left(\frac{1}{\bar{v}_1^n} - \frac{1}{\bar{v}^n}\right) + \theta_2^2\left(\frac{X_{12}'}{\bar{v}^n} - nT\bar{v}_1 Q_{12}\right)\right] - \frac{r_1 c E_1(\phi,\bar{v})}{\bar{v}^{2/3}(\bar{v}^{1/3} - 1)} + \frac{r_1 v^* E_1(\phi,\bar{v})}{kT\bar{v}^{n+1}}\{\phi_1 P_1^* + \phi_2 P_2^* - \phi_1\theta_2 X_{12}'\} \tag{22}$$

and

$$\frac{\Delta\mu_2}{kT} = \ln\phi_2 + (1 - r_2/r_1)\phi_2 + 3r_2\phi_1^2(c_2 - c_1 + 2\phi_2 c_{12}) \ln\sqrt{m_2/m_1} + 3r_2\phi_1^2 c_{12} \ln\{(2\pi m_1 kT)^{1/2}/h(\gamma v^*)^{1/3}(\bar{v}^{1/3} - 1)\} + 3r_2 c_2 \ln\left[\frac{\bar{v}_2^{1/3} - 1}{\bar{v}^{1/3} - 1}\right] + \frac{r_2 v^*}{nkT}\left[P_2^*\left(\frac{1}{\bar{v}_2^n} - \frac{1}{\bar{v}^n}\right) + \theta_1^2\left(\frac{s_2}{s_1}\right)\left(\frac{X_{12}'}{\bar{v}^n} - \bar{v}_1 nTQ_{12}\right)\right] - \frac{r_2 c E_2(\phi,\bar{v})}{\bar{v}^{2/3}(\bar{v}^{1/3} - 1)} + \frac{r_2 v^* E_2(\phi,\bar{v})}{kT\bar{v}^{n+1}}\{\phi_1 P_1^* + \phi_2 P_2^* - \phi_1\theta_2 X_{12}'\} \tag{23}$$

where

$$E_k(\phi,\bar{v}) = \left[\frac{\left(\frac{\bar{r}N_T}{r_k}\right)\frac{\partial\bar{P}}{\partial N_k} - \frac{1}{\bar{T}}\left(\bar{P} + \frac{1}{\bar{v}^{n+1}}\right)\left(\frac{\bar{r}N_T}{r_k}\frac{\partial\bar{T}}{\partial N_k}\right)}{\frac{n+1}{\bar{v}^{n+2}} - \frac{\bar{T}(\bar{v}^{1/3} - 2/3)}{\bar{v}^{5/3}(\bar{v}^{1/3} - 1)^2}}\right] \tag{24}$$

where $k = 1, 2$. The partial derivatives in eq 24 can be evaluated using the equation of state for the mixture. The mixture equation of state can be written in a form identical with the pure component equation of state (eq 7) if the following definitions are made

$$\bar{P} = P/P^* \tag{25}$$

$$P^* = \sum_{i=1}^{n}\phi_i P_i^* - \sum_{j=2}^{n}\sum_{i=1}^{j-1}\phi_i\theta_j X_{ij}' \tag{26}$$

$$\bar{T} = T/T^* \tag{27}$$

and

$$\bar{T} = \frac{1}{P^*}\left[\sum_{i=1}^{n} P_i^*\bar{T}_i\phi_i - \sum_{j=2}^{n}\sum_{i=1}^{j-1}\frac{c_{ij}\phi_i\phi_j kT}{v^*}\right] \tag{28}$$

With these definitions, the mixture equation of state becomes

$$\frac{\bar{P}\bar{v}}{\bar{T}} = \frac{\bar{v}^{1/3}}{\bar{v}^{1/3} - 1} - \frac{1}{\bar{T}\bar{v}^n} \tag{29}$$

Note that the chemical potential of component 1 in a binary mixture using the original Flory–Huggins theory is

$$\frac{\Delta\mu_1}{kT} = \ln\phi_1 + (1 - r_1/r_2)\phi_2 + \phi_2^2 X_{12} \tag{30}$$

By equating the chemical potentials from the two theories, an expression for X_{12}, the Flory–Huggins interaction parameter, can be obtained in terms of the equation of state theory. The result is

$$X_{12} = 3r_1 \ln\sqrt{m_1/m_2}(c_1 - c_2 + 2\phi_1 c_{12}) + 3r_1 c_{12} \ln\{(2\pi m_2 kT)^{1/2}/h(\gamma v^*)^{1/3}(\bar{v}^{1/3} - 1)\} + \frac{3r_1 c_1}{\phi_2^2}\ln\left[\frac{\bar{v}_1^{1/3} - 1}{\bar{v}^{1/3} - 1}\right] + \frac{r_1 v^*}{nkT\phi_2^2}\left[P_1^*\left(\frac{1}{\bar{v}_1^n} - \frac{1}{\bar{v}^n}\right) + \theta_2^2\left(\frac{X_{12}'}{\bar{v}^n} - nT\bar{v}_1 Q_{12}\right)\right] - \frac{r_1 c E_1(\phi,\bar{v})}{\bar{v}^{2/3}(\bar{v}^{1/3} - 1)\phi_2^2} + \frac{r_1 v^* E_1(\phi,\bar{v})}{kT\bar{v}^{n+1}\phi_2^2}\{\phi_1 P_1^* + \phi_2 P_2^* - \phi_1\theta_2 X_{12}'\} \tag{31}$$

Equations 22 and 23 can be used to evaluate the binodal curve for two monodisperse polymers. Setting the chemical potentials of each component equal in both phases, one obtains two equations with two unknowns

$$F_1 = (\Delta\mu_1 - \Delta\mu_1')/kT = 0 \tag{32}$$

$$F_2 = (\Delta\mu_2 - \Delta\mu_2')/kT = 0 \tag{33}$$

These nonlinear algebraic equations can be solved by a number of suitable techniques. The technique used in this study involved finding

$$\min_{\phi}\left\{\frac{F_1^2 + F_2^2}{(\phi_1 - \phi_1')}\right\} \tag{34}$$

using a nonlinear optimization procedure. The denominator in eq 34 avoids the trivial solution, $\phi_1 = \phi_1'$.

C. The Spinodal Curve and Critical Point for Binary Monodisperse Systems. The spinodal curve and the critical point for the binary system can also be computed in a straightforward manner. The spinodal is given by[22]

$$\frac{\partial\Delta\mu_1}{\partial N_1}\Big|_{T,V,\mu_2} = 0 \tag{35}$$

This curve represents the stability limit of a homogeneous sytem to small amplitude composition fluctuations.[23] Substituting eq 22 for $\Delta\mu_1$ and performing the indicated differentiation leads to the spinodal equation for a monodisperse polymer pair

(21) A. J. Bondi, *Phys. Chem.*, 68, 441 (1964).
(22) J. W. Gibbs, "The Scientific Papers of J. Willard Gibbs," Vol. I, Dover Publications, Dover, Del., 1961, pp 130–135.
(23) J. W. Cahn, *J. Chem. Phys.*, 42, 93 (1965).

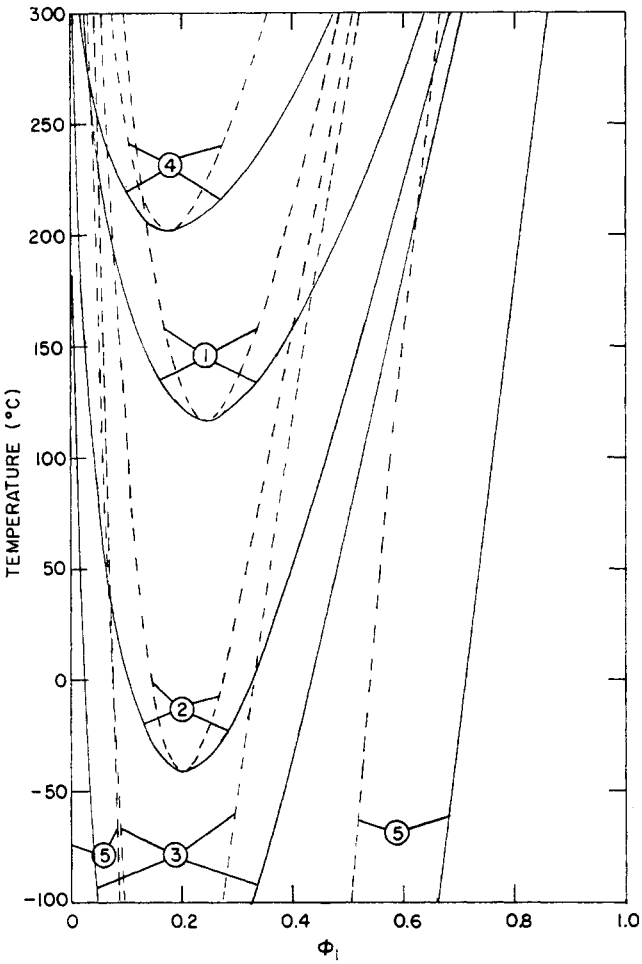

Figure 1. Binodal and spinodal curves illustrating molecular weight effects (phase diagram 1).

Curve No.	Mol Wt
1	$M_1 = 30{,}000$
2	$M_1 = 50{,}000$
3	$M_1 = 80{,}000$
4	$M_2 = 3{,}000$
5	$M_2 = 6{,}000$

$$\frac{1}{r_1\phi_1} + \frac{1}{r_2\phi_2} + 6 \ln \sqrt{m_1/m_2} \times [(c_2 - c_1 + c_{12}(\phi_2 - 2\phi_1)] - 6c_{12} \ln \{(2\pi m_2 kT)^{1/2}/ h(\gamma v^*)^{1/3}(\bar{v}^{1/3} - 1)\} - \frac{2v^*}{nkT}\left(\frac{s_2}{\bar{s}}\right)^2\left(\frac{s_1}{\bar{s}}\right)\left(\frac{X_{12}'}{\bar{v}^n} - nT\bar{v}_1 Q_{12}\right) - H(\phi_1,\bar{v}) \times \left\{\frac{2[c_1 - c_2 + (\phi_1 - \phi_2)c_{12}]}{\bar{v}^{2/3}(\bar{v}^{1/3} - 1)} - \frac{2v^*}{kT\bar{v}^{n+1}}[P_1^* - P_2^* - (\frac{s_2}{\bar{s}})(\phi_2 - \theta_1)X_{12}']\right\} - \left(\frac{\partial H}{\partial \phi_1} + H\frac{\partial H}{\partial \bar{v}}\right)[\frac{c}{\bar{v}^{2/3}(\bar{v}^{1/3} - 1)} - \frac{v^*}{kT\bar{v}^{n+1}} \times (\phi_1 P_1^* + \phi_2 P_2^* - \phi_1\theta_2 X_{12}')] + H^2(\phi_1,\bar{v})\left[\frac{c(\bar{v}^{1/3} - \frac{2}{3})}{\bar{v}^{5/3}(\bar{v}^{1/3} - 1)^2} - \frac{v^*(n+1)}{kT\bar{v}^{n+2}} \times (\phi_1 P_1^* + \phi_2 P_2^* - \phi_1\theta_2 X_{12}')\right] = 0 \quad (36)$$

where the substitution

$$H(\phi_1,\bar{v}) = E_1(\phi,\bar{v})/\phi_2 \quad (37)$$

has been made. The equation for the spinodal possesses either two solutions or no solutions except at the critical point where it possesses a single solution. The critical point is an extremum of the spinodal curve given by the simultaneous solution of eq 35 and

$$\left.\frac{\partial^2 \Delta\mu_1}{\partial N_1^2}\right|_{T,V,\mu_2} = 0 \quad (38)$$

Performing the differentiation indicated by eq 38

$$18c_{12} \ln \sqrt{m_1/m_2} + \frac{6v^*}{nkT}\left(\frac{s_1}{\bar{s}}\right)\left(\frac{s_2}{\bar{s}}\right)^2\left(\frac{\phi_1 - \theta_1}{\phi_1\phi_2}\right)\left(\frac{X_{12}'}{\bar{v}^n} - nT\bar{v}_1 Q_{12}\right) + 3H(\phi_1,\bar{v})\left[\frac{2c_{12}}{\bar{v}^{2/3}(\bar{v}^{1/3} - 1)} - \frac{v^* X_{12}'}{kT\bar{v}^{n+1}}\left(\frac{s_1}{\bar{s}}\right)\left(\frac{s_2}{\bar{s}}\right)\right] - 3H^2(\phi_1,\bar{v})\left[\frac{[c_1 - c_2 - c_{12}(\phi_2 - \phi_1)](\bar{v}^{1/3} - \frac{2}{3})}{\bar{v}^{2/3}(\bar{v}^{1/3} - 1)} - \frac{v^*}{kT\bar{v}^{n+1}}\{P_1^* - P_2^* - \frac{s_2}{\bar{s}}(\phi_2 - \theta_1)X_{12}'\}\right] + 3\left(\frac{\partial H}{\partial \phi_1} + H\frac{\partial H}{\partial \bar{v}}\right)\left[\frac{[c_1 - c_2 - c_{12}(\phi_2 - \phi_1)]}{\bar{v}^{2/3}(\bar{v}^{1/3} - 1)} - \frac{v^*}{kT\bar{v}^{n+1}}\{P_1^* - P_2^* - \frac{s_2}{\bar{s}}(\phi_2 - \theta_1)X_{12}'\}\right] - 3H(\phi_1,\bar{v})\left(\frac{\partial H}{\partial \phi_1} + H\frac{\partial H}{\partial \bar{v}}\right)\left[\frac{c(\bar{v}^{1/3} - \frac{2}{3})}{\bar{v}^{5/3}(\bar{v}^{1/3} - 1)^2} - \frac{v^*(n+1)}{kT\bar{v}^{n+2}}(P_1^*\phi_1 + P_2^*\phi_2 - \phi_1\theta_2 X_{12}')\right] - H^3(\phi_1,\bar{v}) \times \left[\frac{c\{\bar{v}^{1/3}(\bar{v}^{1/3} - 1) - (\bar{v}^{1/3} - \frac{2}{3})[5(\bar{v}^{1/3} - 1) + 2\bar{v}^{1/3}]\}}{3\bar{v}^{8/3}(\bar{v}^{1/3} - 1)^3} + \frac{v^*(n+1)(n+2)}{kT\bar{v}^{n+3}}(P_1^*\phi_1 + P_2^*\phi_2 - \phi_1\theta_2 X_{12}')\right] + \left(\frac{\partial^2 H}{\partial \phi_1^2} + 2H\frac{\partial^2 H}{\partial \phi_1 \partial \bar{v}} + H\left(\frac{\partial H}{\partial \bar{v}}\right)^2 + \frac{\partial H}{\partial \bar{v}}\frac{\partial H}{\partial \phi_1} + H^2\frac{\partial^2 H}{\partial \bar{v}^2}\right) \times \left[\frac{c}{\bar{v}^{2/3}(\bar{v}^{1/3} - 1)} - \frac{v^*}{kT\bar{v}^{n+1}} \times (P_1^*\phi_1 + P_2^*\phi_2 - \phi_1\theta_2 X_{12}')\right] = \frac{1}{r_2\phi_2^2} - \frac{1}{r_1\phi_1^2} \quad (39)$$

The temperature and composition at the critical point can be obtained by solving the spinodal and critical point equations (eq 36 and 39) simultaneously.

D. The Spinodal Curve and Critical Point for Binary Polydisperse Systems. It is also possible to extend the Flory theory to polydisperse systems using the results of Koningsveld *et al.*[9] This can be done by expressing the free energy of mixing from eq 16 as

$$Z = \left(\frac{\Delta F^m/\bar{r}N_T}{kT}\right) = \sum_{i=1}^{n}\frac{\phi_i}{r_i} \ln \phi_i + \phi_1^0\phi_2^0 X_{12} \quad (40)$$

where

$$\phi_1^0 = \sum_{i=1}^{m}\phi_i$$

$$\phi_2^0 = \sum_{i=m+1}^{n}\phi_i$$

The summations for ϕ_1^0 and ϕ_2^0 extend over all chain lengths of polymers 1 and 2 in the mixture. Hence, ϕ_1^0

and ϕ_2^0 represent the quasi-binary compositions of polymers 1 and 2, respectively. By comparing eq 16 with eq 40, the generalized Flory–Huggins interaction parameter, X_{12}, becomes

$$X_{12} = \frac{1}{\bar{r}_1^0 N_1^0 \phi_2^0}\left\{\sum_{i=1}^{n} 3r_i N_i (c_i - c) \times \ln\{(2\pi m_i kT)^{1/2}/h\} + 3\bar{r}N_T \sum_{j=2}^{n}\sum_{i=1}^{j-1} \phi_i \phi_j c_{ij} \times \ln\{(\gamma v^*)^{1/3}(\bar{v}^{1/3} - 1)\} + 3\sum_{i=1}^{n} r_i N_i c_i \times \ln\left[\frac{\bar{v}_i^{1/3} - 1}{\bar{v}^{1/3} - 1}\right] + \frac{\bar{r}N_T v^*}{nkT}\left[\sum_{i=1}^{n}\phi_i P_i^*\left(\frac{1}{\bar{v}_i^n} - \frac{1}{\bar{v}^n}\right) + \sum_{j=2}^{n}\sum_{i=1}^{j-1}\left(\frac{\phi_i \theta_j X_{ij}'}{\bar{v}^n} - nT\bar{v}_i \phi_i \theta_j Q_{ij}\right)\right]\right\} \quad (41)$$

where

$$N_1^0 = \sum_{i=1}^{m} N_i$$

$$\bar{r}_1^0 = \sum_{i=1}^{m} N_i r_i / N_1^0$$

This equation can be simplified for a binary polydisperse polymer pair by recognizing that the number of segments per molecule varies but that the chemical composition of the segments must be either of two types. Hence, a number of equalities can be expected to apply provided the pure component properties are independent of chain length. These equalities are summarized in Table I. Meisner[24] has shown that the pure component properties are relatively insensitive to chain length for chain lengths greater than $r_i = 100$.

When considerable amounts of low molecular weight species are present, the equalities assumed in Table I would be in error. In addition, the degrees of freedom parameter, the interaction parameter and the entropic correction factor should be near zero for the same polymer at moderately high chain lengths where end group corrections are insignificant. Of course, for highly branched polymers, these parameters may assume significant nonzero values. When the end group corrections can be ignored, the only parameters which remain are those for molecularly different segments. These parameters then reduce to the three fixed constants, $\bar{c}_{12}$, $\bar{X}_{12}$, and $\bar{Q}_{12}$ of Table I.

With these equalities X_{12} becomes

$$X_{12} = \frac{1}{\phi_1^0 \phi_2^0}\left\{3\phi_1^0(c_1 - \bar{c}) \ln\{(2\pi m_1 kT)^{1/2}/h\} + 3\phi_2^0(c_2 - \bar{c}) \ln\{(2\pi m_2 kT)^{1/2}/h\} + 3\phi_1^0\phi_2^0\bar{c}_{12} \ln\{(\gamma v^*)^{1/3}(\bar{v}^{1/3} - 1)\} + 3c_1\phi_1^0 \ln\left[\frac{\bar{v}_1^{1/3} - 1}{\bar{v}^{1/3} - 1}\right] + 3c_2\phi_2^0 \ln\left[\frac{\bar{v}_2^{1/3} - 1}{\bar{v}^{1/3} - 1}\right] + \frac{v^*}{nkT}\left[P_1^*\left(\frac{1}{\bar{v}_1^n} - \frac{1}{\bar{v}^n}\right)\phi_1^0 + P_2^*\left(\frac{1}{\bar{v}_2^n} - \frac{1}{\bar{v}^n}\right)\phi_2^0 + \phi_1^0\theta_2^0\left(\frac{\bar{X}_{12}}{\bar{v}^n} - nT\bar{v}_1\bar{Q}_{12}\right)\right]\right\} \quad (42)$$

Koningsveld *et al.*[9] have shown that the quasi-binary spinodal and critical point equations for two polydisperse polymers can be evaluated in terms of this X_{12}. The spinodal equation is given by

$$2X_{12} - 2(\phi_2^0 - \phi_1^0)\frac{\partial X_{12}}{\partial \phi_1^0} - \phi_1^0\phi_2^0\frac{\partial^2 X_{12}}{\partial \phi_1^{02}} = \frac{1}{\phi_1^0 \bar{r}_{w_1}} + \frac{1}{\phi_2^0 \bar{r}_{w_2}} \quad (43)$$

where

$$\bar{r}_{w_1} = \sum_{i=1}^{m} \phi_i r_i / \phi_1^0$$

$$\bar{r}_{w_2} = \sum_{i=m+1}^{n} \phi_i r_i / \phi_2^0$$

The consolate state conditions require the simultaneous satisfaction of

$$-6\frac{\partial X_{12}}{\partial \phi_1^0} + 3(\phi_2^0 - \phi_1^0)\frac{\partial^2 X_{12}}{\partial \phi_1^{02}} + \phi_1^0\phi_2^0\frac{\partial X_{12}}{\partial \phi_1^{03}} = \frac{\bar{r}z_1}{\bar{r}_{w_1}^2\phi_1^{02}} - \frac{\bar{r}z_2}{\bar{r}_{w_2}^2\phi_2^{02}} \quad (44)$$

where

$$\bar{r}_{z_1} = \frac{1}{\phi_1^0 \bar{r}_{w_1}}\sum_{i=1}^{m}\phi_i r_i^2$$

$$\bar{r}_{z_2} = \frac{1}{\phi_2^0 \bar{r}_{w_2}}\sum_{i=m+1}^{n}\phi_i r_i^2$$

The evaluation of the partial derivatives in eq 43 leads to a quasi-binary spinodal equation which is algebraically identical with the monodisperse spinodal (eq 36) if the following substitutions are made

$\phi_1 \rightarrow \phi_1^0$	$c_{12} \rightarrow \bar{c}_{12}$
$\phi_2 \rightarrow \phi_2^0$	$c \rightarrow \bar{c}$
$r_1 \rightarrow \bar{r}_{w_1}$	$X_{12}' \rightarrow \bar{X}_{12}$
$r_2 \rightarrow \bar{r}_{w_2}$	$Q_{12} \rightarrow \bar{Q}_{12}$

Hence, the analysis shows that the quasi-binary spinodal curves are identical to the binary spinodal curves for monodisperse polymer pairs if the chain length of each component is replaced by the weight average chain length.

In a similar manner, the left-hand side of eq 44 reduces to an algebraic form which is identical to the left-hand side of eq 39 when the above substitutions are made. The right side of eq 39 and 44 differ because of chain-length distribution effects. The critical temperature and composition are obtained by satisfying eq 43 and 44 simultaneously. Hence, the critical point must lie on the spinodal curve. The exact location is determined by the z average and the weight-averaged chain length statistics for each polymer.

Discussion

With the theory developed in the previous section, it is possible to compute binodal and spinodal curves for representative polymer pairs. These calculations have been made for two basic hypothetical types of phase diagrams using pure component equation of state parameters which have been measured for real polymeric components. This approach has been taken because the complex structure of eq 22, 23, and 36 makes it difficult to estimate the effects of the various parameters using any other procedure. The general structure of the phase diagrams is discussed in

(24) J. Meisner, *Ind. Eng. Chem., Fundam.*, 11, 83 (1972).

Table II
Base Case Parameters for Simulated Polymer-Polymer Phase Diagrams

Component	M_i	$M(m_i)$	ρ (g/cm^3)	α (°K^{-1})	γ (atm/°K)	n	Temp (°C)
			a. Pure Component Properties				
1	50,000	104	1.005[a]	5.80×10^{-4}	8.47	1.0	135
2	4,000	58	1.055[a]	7.23×10^{-4}	7.24	1.0	135
			Mixture properties: $c_{12} = X_{12}' = Q_{12} = 0$; $s_1/s_2 = 1.56$[b]				
			b. Pure Component Properties				
1	100,000	104	1.005	5.80×10^{-4}	8.47	1.0	135
2	100,000	104	1.005	6.15×10^{-4}	8.47	1.0	135
			Mixture properties: $c_{12} = X_{12}' = Q_{12} = 0$; $s_1/s_2 = 1.0$				

[a] Because of interest in the polystyrene-poly(vinylmethyl ether) system, the density and molecular weights of a "mer" were arbitrarily set to that of polystyrene and poly(vinylmethyl ether), respectively. [b] Estimated using Bondi's technique.[21]

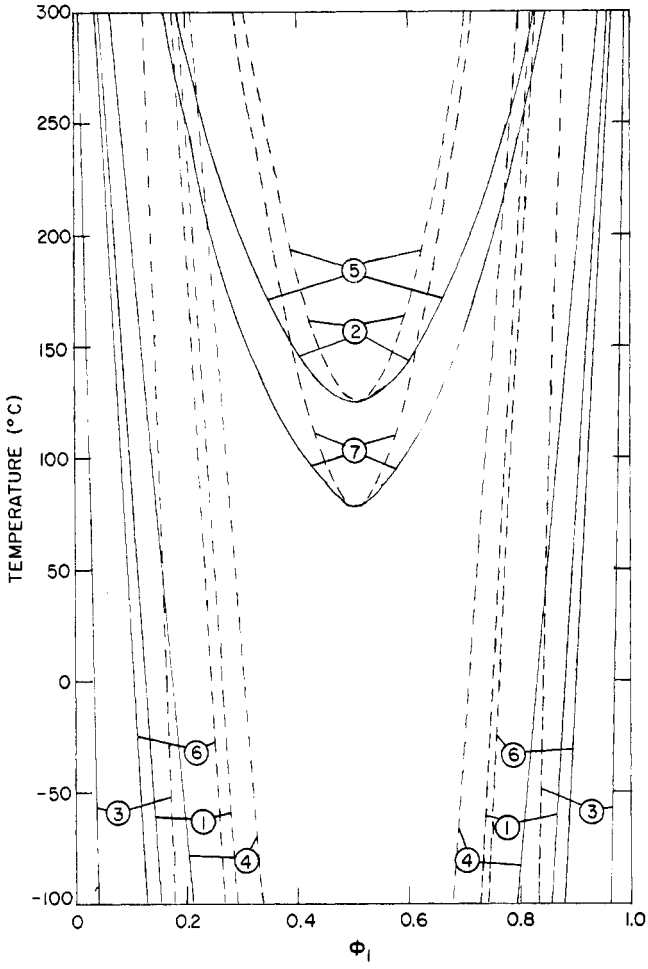

Figure 2. Effects of molecular weight and the thermal expansion coefficient (phase diagram 2), $\alpha_1 = 0.580 \times 10^{-3}$ °K^{-1}.

Curve No.	Molecular Weight	α_2 (°K$^{-1} \times 10^3$)	Rel % Diff $(\alpha_2 - \alpha_1) \times 100/\alpha_1$
1	$M_1 = M_2 = 50{,}000$	0.640	10.3
2	$M_1 = M_2 = 50{,}000$	0.630	8.6
3	$M_1 = M_2 = 100{,}000$	0.630	8.6
4	$M_1 = M_2 = 100{,}000$	0.620	6.9
5	$M_1 = M_2 = 100{,}000$	0.615	6.0
6	$M_1 = M_2 = 200{,}000$	0.610	5.2
7	$M_1 = M_2 = 200{,}000$	0.605	4.3

some detail. By making perturbations in properties around base case values, the effect of each parameter on mutual solubility has been ascertained. Parameters varied in this fashion include chain length, thermal expansion coefficient, thermal pressure coefficient, and the various empirical mixture parameters.

The effects of pressure and polydispersity on the phase equilibria can also be predicted using the Flory theory. Calculations have been made for selected cases to illustrate the qualitative effects of these variables.

A. Thermodynamic Parameters for Two Basic Systems. It is of interest to see if the generalized Flory theory can explain the lcst behavior which has been observed for several polymer pairs. To accomplish this, spinodal and binodal curves have been computed for two types of simulated polymer pairs possessing realistic values of the equation of state parameters. For the first system, the equation of state parameters of the two polymers were allowed to assume values which differ as much as possible within reasonable limits. If equation of state effects are at all significant, this type of system should show the greatest nonideality. Toward this end, the equation of state parameters of polystyrene and polyethylene[25,20] were used for this first basic system. The mixture parameters (c_{12}, X_{12}', Q_{12}) were set identically with zero at first so that the equation of state effects could be studied separately. The base case values of the parameters used in the calculations are summarized in Table IIa. The molecular weight of component 1 was set arbitrarily to 50,000. The molecular weight of component 2 was adjusted so that the critical point temperature fell into a temperature range of interest (−100 to 300°). Many phase diagrams were then computed corresponding to small perturbations in pure component and mixture parameters around the base case.

For the second basic type of simulated polymer-polymer system, both polymers were assumed to have equal and high molecular weight. The pure component properties of polystyrene were again taken for component 1. Small perturbations in the equation of state and mixture properties were then assumed for the second component so that the effects of these parameters could be studied one at a time. The base case parameters for phase diagram type 2 are summarized in Table IIb.

B. The General Lcst Behavior. The results of the computations show that polymer-polymer mutual solubility decreases with increases in temperature for all cases when $X_{12}' \leq 0$. (The case when $X_{12}' > 0$ is discussed in more detail in a later section.) Lcst behavior is the norm for these polymeric systems. The reason for this behavior lies in the significance of the equation of state effects for these high molecular weight systems. Because both components have long chain lengths, the combinatorial entropy contribution to the free energy of mixing is small. Mutual solubility of one component in another is not possible unless the interaction energy term is a small positive number or even negative, *i.e.*, 1-2 interactions stronger than 1-1, 2-2 interactions. Under these conditions, the equation of state

(25) H. Höcker, G. J. Blake, and P. J. Flory, *Trans. Faraday Soc.*, 67, 2251 (1971).

effects control the basic structure of the mutual solubility relationships.

These equation of state effects lead to a negative excess volume of mixing when one polymeric liquid is more expanded than the other (*i.e.*, $\tilde{v}_1 > \tilde{v}_2$). The free volume of the homogeneous system is less than that of the demixed system. Such a decrease in free volume often leads to an exothermic heat of mixing and a negative excess entropy of dilution. Indeed, Haase[26] has shown that both $\Delta E^m < 0$ and $\Delta S^E < 0$ unless an inflection point exists in the concentration dependence of these functions at the critical temperature. Since such inflection points cannot be precluded in general, the negativity of these functions cannot be regarded as necessary conditions for an lcst. For all of the cases reported in this work, the computed excess volume of mixing was negative at the lcst. The excess entropy of mixing was negative in all cases except when the chain length of one component was much greater than the other. This type system approaches the polymer–solvent case. The internal energy of mixing was usually negative although there were some exceptions for $X_{12}' > 0$ and at high pressures.

For a monodisperse polymer pair, a comparison of the critical point composition using the equation of state theory (from eq 36 and 39) can be made with an estimate of this composition using the Flory–Huggins approximation

$$\phi_1(\text{crit})/\text{F–H} = \frac{1}{1 + (r_1/r_2)^{1/2}} \tag{45}$$

This comparison has been made. The results show that the Flory–Huggins approximation can be used to estimate the critical composition in most cases to within 10%. For phase diagram 1 (Table IIa), the estimate of ϕ_1 was generally too high. The reverse was true for phase diagram 2 (Table IIb). Not too surprisingly, better approximations are obtained when the two polymers have nearly identical equation of state parameters. That is, the approximation for phase diagram 2 was usually better than that for phase diagram 1. The greatest error (> 10%) in the Flory–Huggins approximation occurs when both the thermal expansion coefficient and the thermal pressure coefficient of each polymer differ considerably in value.

Just as the Flory–Huggins approximation can be used to estimate the critical composition, it can also be used to estimate the critical X_{12} parameter given by eq 31. The Flory–Huggins approximation is

$$X_{12}(\text{crit})/\text{F–H} = \frac{(1 + (r_1/r_2)^{1/2})^2}{2(r_1/r_2)} \tag{46}$$

When this comparison is made, the Flory–Huggins approximation is found to give a poor estimate of X_{12}(crit) for phase diagram 1 where the differences in equation of state parameters are large. The Flory–Huggins approximation, however, provides a reasonable estimate (within 4%) for phase diagram 2 where equation of state differences are small. In this latter case, eq 45, 46, and 31 can be used to estimate both the critical composition and the critical temperature with fair accuracy. Equation 45 is used to estimate ϕ_1(crit). Equation 46 provides an estimate of X_{12}(crit). When both of these values are substituted into eq 31, the critical temperature can be determined implicitly. This approximation procedure can be used only when equation of state parameter differences are small. When larger differences exist, eq 36 and 39 must be solved simultaneously.

(26) R. Haase, *Discuss. Faraday Soc.*, **15**, 270 (1953).

C. The Effect of Model Parameters on the Thermodynamic Phase Diagrams. The binodal and spinodal curves have been computed using the equation of state theory so that the qualitative effects of model parameters on phase behavior can be determined. These effects are discussed in the section below. Included in the discussion are the effects of molecular weight, equation of state parameters, the energy interaction parameter, and other model parameters which have been found to be of secondary importance.

a. The Effect of Molecular Weight. Molecular weight effects are accounted for in the theory in terms of chain length effects for monodisperse, unbranched polymers. The chain length of component 1 has been arbitrarily defined as

$$r_1 = \frac{M_1}{M_{m1}} \tag{47}$$

the ratio of the polymer molecular weight to the "mer" molecular weight. Based upon this assumption, the chain length of every other polymer species becomes

$$r_i = r_1 V_i^*/V_1^* \tag{48}$$

Hence, the chain-length ratios are proportional to hard core molecular volume ratios.

The effect of varying the molecular weights of components 1 and 2 for phase diagram 1 is shown in Figure 1. In the figure, the binodals are indicated with solid lines whereas the spinodals are drawn as dashed lines. This figure illustrates the general lcst behavior. As the molecular weight of either component increases, the mutual solubility of the two polymers decreases. This is expected since the combinational entropy term in the free energy of mixing decreases monotonically as the molecular weight of either component increases. The same general behavior is also found to occur for phase diagram 2 as the molecular weights of both components are changed simultaneously (Figure 2). These curves also illustrate a general skewness of the binodal and spinodal curves when the chain lengths of the two polymers differ considerably. The critical composition gradually shifts to the left as r_1/r_2 decreases.

b. The Effect of the Thermal Expansion Coefficient. Polymer–polymer solubility is more sensitive to changes in the thermal expansion coefficient than it is to changes in the thermal pressure coefficient. As eq 11, 12, and 13 indicate, changes in the thermal expansion coefficient cause changes in all three equations of state parameters. A 6% increase in α leads to a 4.6% decrease in T^*, a 2.0% increase in P^*, and a 1.0% decrease in v^* at a temperature of 300°K.

Figure 2 shows the effect of small changes in the thermal expansion coefficient of component 2 for phase diagram 2. This figure shows that two polymers having molecular weights of 200,000 (chain length ~2000) require differences in thermal expansion coefficients of 4% or less in order to show significant mutual solubility. Even at molecular weights as low as 50,000, differences in thermal expansion coefficients as small as 10% can lead to virtually complete immiscibility. Furthermore, in these high molecular weight cases very small perturbations in the thermal expansion coefficient of one component cause large shifts in the positions of the phase boundaries. An example for two components having molecular weights of 100,000 is shown in the shift of the binodal and spinodal curves 3, 4, and 5 of Figure 2. These shifts are caused by ~1.6 and ~0.8% changes in the thermal expansion coefficients of component 2 between curves ¾ and ⅘, respectively.

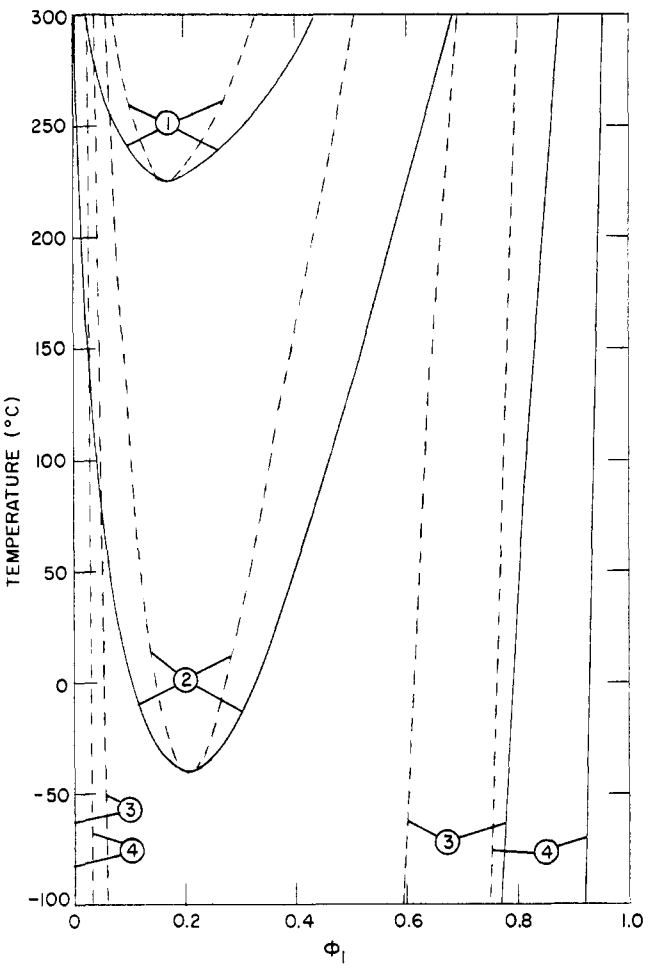

Figure 3. Effect of thermal pressure coefficient (phase diagram 1).

Curve No.	γ_2 (atm/°K)
1	6.50
2	7.24
3	8.47
4	10.00

Similar results are found for phase diagram 1. Larger differences in thermal expansion coefficients in the neighborhood of 20% are required in this case where one component is much lower in molecular weight (*i.e.*, M_2 = 4000).

c. The Effect of the Thermal Pressure Coefficient. As eq 11-13 illustrate, changes in the thermal pressure coefficient cause correspondingly proportional changes in P^* only. The other equation of state parameters are unaffected. The effect of variations in γ_2 is illustrated in Figure 3 for phase diagram 1. These results show that equation of state differences caused by $\alpha_1 < \alpha_2$ can be at least partially compensated by reducing γ_2 in comparison to γ_1. Evaluation of the equation of state parameters shows that differences in T_i^* and $\tilde{v}_i$ can be partially compensated by increasing further the differences in P_i^*. Figure 3 shows that a 10% decrease in γ_2 from 7.24 to 6.50 atm per °K leads to an increase in the critical temperature of over 250°.

A similar effect is also found if γ_1 is varied with all other parameters fixed. In this case, increases in γ_1 (with the resulting increase in $\gamma_1 - \gamma_2$) also lead to increases in mutual solubility of the two components. The same qualitative behavior also occurs for phase diagram 2. In this case, because both components are high molecular weight, smaller changes in the thermal pressure coefficient are needed to cause shifts in the critical temperature comparable with the shifts found for phase diagram 1.

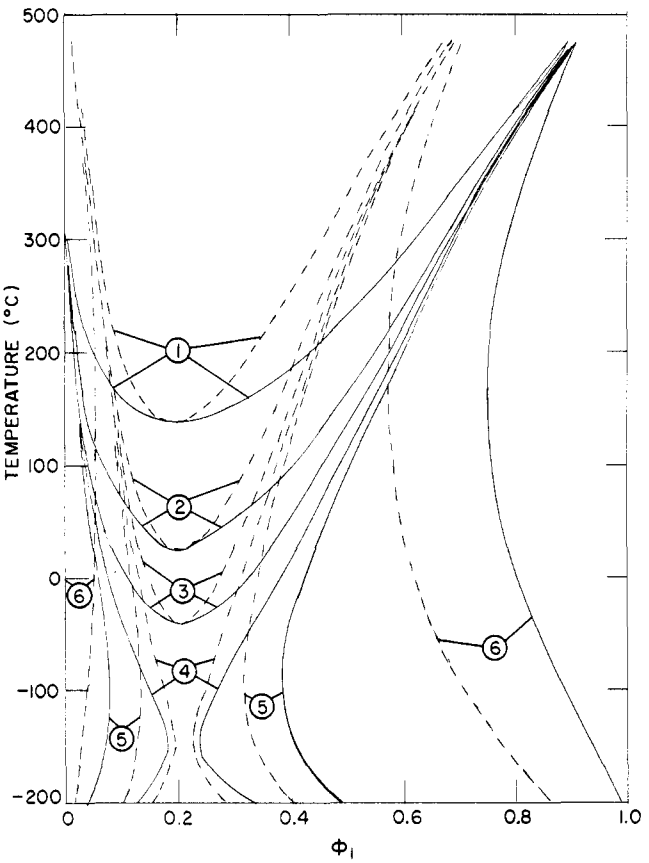

Figure 4. Effect of interaction energy parameter (phase diagram 1).

Curve No.	X_{12}' (cal/cm³)
1	−0.050
2	−0.100
3	0.0
4	0.005
5	0.010
6	0.100

d. The Effect of the Energy Interaction Parameter. Strictly speaking, the theoretical development is restricted to mixtures of nonpolar molecules. Obviously, it would be desirable to extend this treatment to polar molecules and even to those for which specific segmental interactions exist (like hydrogen-bonding or acid-base interactions). The extension can be made qualitatively through the use of the interaction parameter. Arbitrarily, the interaction parameter is allowed to assume both positive and negative values. Positive values of this parameter correspond to cases where 1-1, 2-2 type segmental interactions are stronger than 1-2 interactions. When 1-2 interactions dominate over 1-1, 2-2 interactions, the interaction parameter assumes negative values. This latter case should be anticipated when strong hydrogen bonding or acid-base-type interactions exist. In all probability, the functional dependence of this term upon temperature, pressure, and composition will be incorrect when applied to a specific case. The functional dependencies of X_{12}' are ignored in this study. Fortunately, the qualitative effect of this term can be seen without the addition of such complexities.

Figure 4 shows the effect of adding nonzero values of the interaction energy parameter for phase diagram 1. The temperature range has been extended to illustrate the phase behavior over a broader range. When negative values of X_{12}' are introduced, the qualitative phase behavior remains unchanged. The critical temperature is raised and the binodal and spinodal curves tend to flatten out.

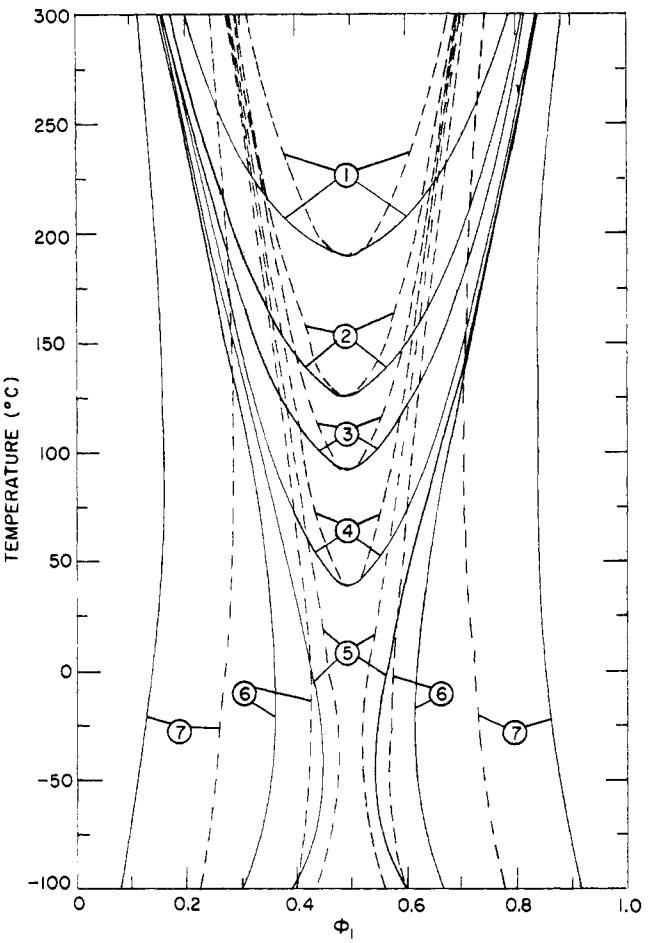

Figure 5. Effect of interaction energy parameter (phase diagram 2).

Curve No.	X_{12}' (cal/cm³)
1	−0.00150
2	0.0
3	0.00050
4	0.00100
5	0.00125
6	0.00150
7	0.00500

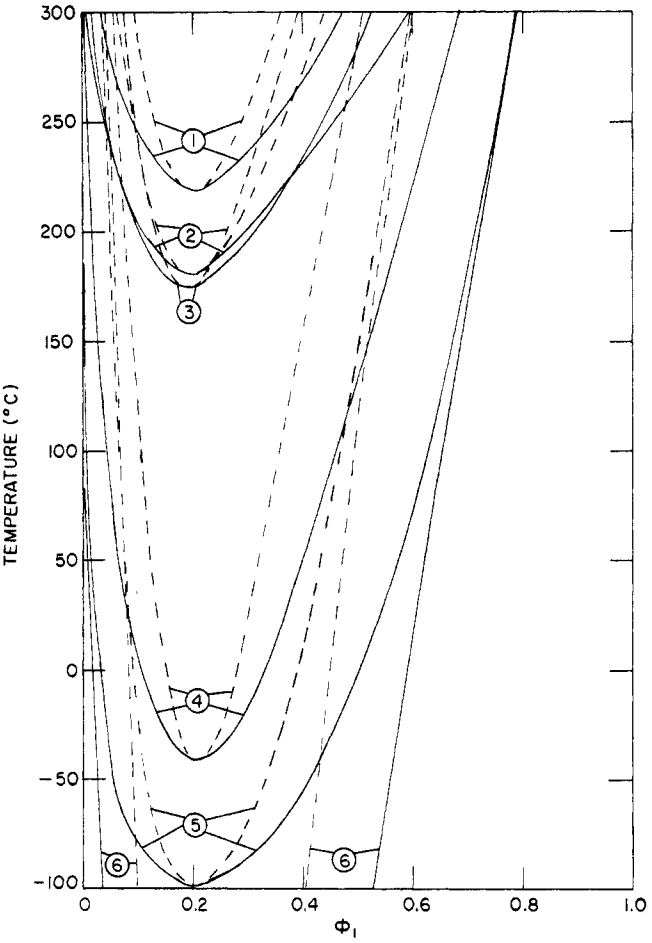

Figure 6. Effect of c_{12}, Q_{12}, and n (phase diagram 1).

Curve No.	c_{12}	Q_{12} (cal/(cm³ − °K))	n
1	−0.001	0.0	1.0
2	0.0	0.0	1.25
3	0.0	0.0001	1.0
4	0.0	0.0	1.0
5	0.001	0.0	1.0
6	0.0	−0.0001	1.0

Small positive values of X_{12}' lead to both ucst and lcst behavior. For the values of X_{12}' assumed in Figure 4, the two critical points have already merged to give skewed hourglass-shaped binodal and spinodal curves. In this case, mutual solubility increases as temperature is raised from absolute zero, but at higher temperatures, the solubility tends to decrease. The temperature where the lcst and the ucst merge is a function of the magnitude difference of the component thermal expansion coefficients. For the thermal expansion coefficients of phase diagram 1, Figure 4 indicates that this temperature is around −150°. However, when the thermal expansion coefficient of component 2 is reduced from 7.23×10^{-4} °K^{-1} to 6.80×10^{-4} °K^{-1} the ucst and the lcst merge closer to −25°.

Figure 5 shows that the same qualitative behavior occurs for phase diagram 2. In this case, the ucst and the lcst also merge at temperatures between −50 and 0°. Although not shown on this plot, curves 3 and 4 also have ucst-type binodals at lower temperatures. The ucst for curve 4, for example, is −131.6°. Because the combinational entropy of mixing is much smaller for this system, positive interaction energy parameters smaller by nearly a factor of five are sufficient to lead to partial solubility over the entire temperature range.

These sets of curves point out two additional aspects of polymer-polymer solubility. (1) Specific interactions leading to negative X_{12}' enhance solubility by raising the critical temperature and flattening the binodal and spinodal curves on a $T - \phi$ diagram. Larger equation of state differences can be tolerated without incompatibility when $X_{12}' < 0$. A situation of this type can probably be expected for most compatible polymer pairs of practical significance. (2) The simultaneous occurrence of an lcst and a ucst should be rare for polymer-polymer systems. The range of X_{12}' values over which it can occur is small and the temperature where the two merge is generally at or below 0°. This last statement is subject to the restrictions of the model, of course. Whenever significant temperature dependence of X_{12}' is included in the model, it may be possible to obtain a ucst at a significantly higher temperature. The general picture of the dominant lcst behavior with much less ucst behavior clearly emerges from these results.

e. The Effect of c_{12}, Q_{12}, and n. These parameters are lumped together because they do not change the qualitative view of polymer-polymer thermodynamic behavior already obtained from results using $c_{12} = 0$, $Q_{12} = 0$, and $n = 1.0$. Figure 6 illustrates the effects obtained by adding each of the above parameters to the model, using phase diagram 1 as the base case. The qualitative effect of each of these variables is reviewed in Table III. As the table shows, negative values of c_{12}, the degrees of freedom pa-

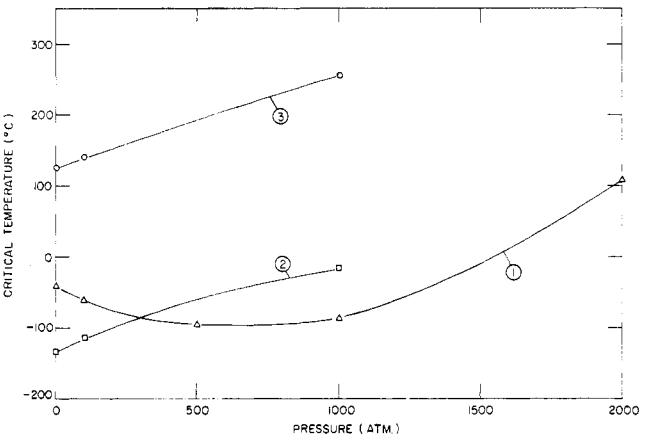

Figure 7. Critical temperature *vs.* pressure

Curve No.	Phase Diagram
1	1
2	2
3	1 – equal $\gamma_i - M_1 = 3000$

Table III
Qualitative Effect of Secondary Parameters on Mutual Solubility

Parameter	Positive Value	Negative Value	Crit Soln Temp Behavior
c_{12}	Decreases solubility	Increases solubility	Unchanged
Q_{12}	Increases solubility	Decreases solubility	Positive, unchanged Negative, both lcst and ucst
n	Increases solubility	Decreases solubility	Unchanged

rameter, increase solubility; positive values reduce solubility. In both cases, the lcst behavior remains. The entropic parameter, Q_{12}, enters into the free energy of mixing in a manner very similar to the energy interaction parameter. In this case, positive values enhance solubility. Negative values can lead to the simultaneous lcst and ucst, although for the case shown in Figure 6, decreasing solubility with temperature occurs over the full temperature range. Finally, the effect of increasing n (volume dependence of the lattice energy, eq 4) from 1.0 to 1.25 is illustrated. Compatibility is enhanced by this change; the binodal and spinodal curves are also flattened somewhat.

D. The Effect of Pressure on Solubility. As pressure is increased, errors of increasing magnitude can be anticipated in both the pure component and mixture equations of state because of the simple monotonic dependence of the lattice energy with distance (eq 4) assumed in the model. If this fault in the model is ignored, it is possible to predict the effect of pressure on polymer–polymer solubility. By using the equation of state thermodynamics, the pressure effects are illustrated in Figure 7 for three different sets of parameters. This figure shows the effect of applied pressure on the critical temperature. Curve 1 illustrates the effect of applied pressure for phase diagram 1. Surprisingly, the critical temperature first decreases until pressures in the neighborhood of 700 atm are reached. The application of still larger pressures causes the critical temperature to then increase. Curve 2 shows the effect of pressure for phase diagram 2. In this case, the critical temperature increases monotonically with pressure.

An explanation of the anomolous behavior obtained for phase diagram 1 can be made in the following way. Curve 3 shows the effect of pressure for a modified phase diagram 1. The thermal pressure coefficients of both components have been set equal to 7.24 atm/°K. The molecular weight of component 2 was also reduced to 3000 so that the atmospheric pressure critical point fell into a reasonable temperature range. Using these parameters, the critical temperature again increased monotonically with applied pressure. Hence, the anomolous behavior for phase diagram 1 (curve 1) is caused by the difference in thermal pressure coefficients (and P_1^*) for the two components.

When the binodal and spinodal curves for these higher pressure cases were plotted on $T - \phi$ diagrams, the solubility and stability limits tend to be compressed somewhat. This makes the curves much steeper at higher pressures. Thus, even though the critical temperature of phase diagram 1 is lower at 1000 atm than it is at 1 atm, the mutual solubility of the two polymers is actually greater at 1000 atm for temperatures above 150° because the binodal curves for the two pressures cross over one another at this temperature. Similar compression effects occur for phase diagram 2, although in this case the binodal and spinodal curves never cross over one another because the critical temperature increases monotonically with pressure.

E. Molecular Weight Distribution Effects. The discussion has been restricted thus far to monodisperse polymer pairs. By using eq 36 and 39 with the appropriate substitution from eq 43 and 44 for polydisperse systems, the results can be generalized so that molecular weight distribution effects can be analyzed. All of the spinodal curves presented above remain unchanged so long as the weight-average chain length is substituted in place of the monodisperse chain length for each species. Of course, one is actually referring to a quasi-binary spinodal where all of the components of the same molecular species but different chain length are considered as one component.

When a distribution of molecular weight exists, the consolate state no longer necessarily exists at the extremum of the spinodal curve. Instead, it may lie on either ascending branch (for an lcst) of the quasi-binary spinodal curve. The position of the critical point depends only upon the weight average and the z-average chain length of each component. For fixed weight-average chain length and hence, fixed quasi-binary spinodal curve, the only molecular weight distribution statistic of significance is

$$a_i = \frac{\bar{r}_{z_i}}{\bar{r}_{w_i}}, \qquad (47)$$

the ratio of the z-average to weight-average chain length of each component.

The effect of a distribution of molecular weight on the critical point is illustrated for phase diagrams 1 and 2 in Figure 8. As before, the spinodal curves are represented by dashed lines. The critical points for various values of a_1 and a_2 are shown. These results show that the critical point shifts very little from the monodisperse critical point no matter how great the polydispersity so long as both components have equal values of a_i. When $a_2 > a_1$, the critical point shifts to the left ascending branch of the spinodal; *i.e.*, higher ϕ_2. Conversely, when $a_1 > a_2$, it shifts to the right ascending branch – higher ϕ_1. The results show that the shift in the critical point can be quite dramatic when one polymer is considerably more polydisperse than the other.

The calculation of the binodal curves for polydisperse polymer pairs is considerably more difficult than the calculation of the spinodal and the critical point, particularly when both components are polydisperse.[9] For this reason,

Table IV
Molecular Weight Distribution Statistics of Polymers

Polymer	Commercial Code	M_n	M_w	M_z	M_w/M_n	M_z/M_w
	a. Experimental System 1					
Polystyrene	Union Carbide—SMD-3500	78,400	236,600	455,000	3.02	1.92
Poly(vinylmethyl ether)	GAF—Gantrez—M093	7,700	13,320	21,800	1.73	1.63
	b. Experimental System 2					
SAN copolymer	Union Carbide—RMD-4511 (28% AN)	88,600	223,200	679,600	2.06	3.05
Polycaprolactone	Union Carbide—PCL-700	2,240	35,000	61,100	15.6	1.75

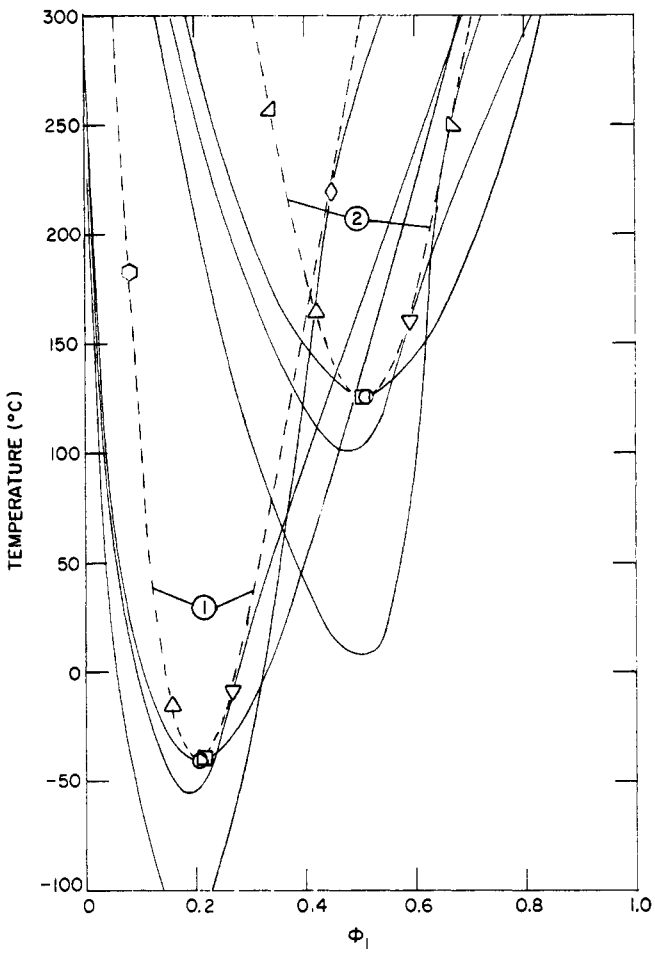

Figure 8. Effect of molecular weight distribution, spinodal curves, and critical points for varying a_1 and a_2, cloud point curves simulated except when $a_1 = a_2 = 1.0$; curves 1 and 2 represent phase diagrams 1 and 2, respectively.

Symbol	a_1	a_2	a_1/a_2
○	1.0	1.0	1.0
□	10.0	10.0	1.0
△	1.0	2.0	0.5
▽	2.0	1.0	2.0
◁	1.0	4.0	0.25
▷	4.0	1.0	4.0
⬡	1.0	10.0	0.10
◇	10.0	1.0	10.0

only some illustrative cloud point curves are drawn (as solid lines) in Figure 8. These cloud point curves (CPC) correspond to the point of incipient phase separation when a homogeneous specimen is heated at an infinitesimally slow rate. For monodisperse polymers, the CPC also corresponds to the binodal since the composition on the opposite ascending branch of the binodal curve is in equilibrium with the matrix composition at the cloud point.

For polydisperse polymer pairs, this is not true. That is, the two cloud point compositions at any given temperature are not generally in equilibrium with one another. The magnitude of the error in assuming the two cloud points to be in equilibrium is a function of the polydispersity of the two polymers. Even with these complications, the critical point must still be unique since the equilibrium compositions of the two phases must become identical at that point. Furthermore, as with the true binary, the CPC and the spinodal have a common tangent at the critical point. Based upon this knowledge, a few qualitative CPC's have been drawn on Figure 8. It should be noted that the CPC can shift a considerable distance below the extremum of the spinodal when one polymer is more polydisperse than the other. The necessity of forming a common tangent with the spinodal can also lead to a distinct dimple in the CPC at the critical point.

Experimental Section

Cloud point curves have been measured for two polymer-polymer systems so that a qualitative comparison with the theory can be made. These systems are the polystyrene (PS)-poly(vinylmethyl ether) (PVME) and the styrene-acrylonitrile copolymer (SAN)-polycaprolactone (PCL) systems. The lcst behavior of the former system was recently presented by Bank, Leffingwell, and Thies.[27] The molecular weight distribution statistics for these polymers were determined by gel permeation chromatography. Results are presented in Table IV. The weight-average molecular weight of component 1 is significantly greater than that of component 2 for both of these systems. Hence, some skewness of the binodal and spinodal curves toward low weight fractions of the high molecular weight component should be expected. In addition, the z-average to weight-average molecular weight ratio of the two components is 1.75:1 for the second system. For this system, the critical point should be shifted from the extremum of the CPC to higher weight fractions of the component having the higher M_z/M_w (SAN copolymer).

A. Experimental Procedure. Each of the polymers used in this study is a commercial material (Table IV). Without any purification steps, solutions of PS-PVME in toluene and SAN-PCL in 1,2-dichloroethane were cast onto microscope slides. The solvent was evaporated to obtain thin 1-2-mil films. These films were then dried for times exceeding 24 hr at temperatures between the glass transition temperature (or the crystallization temperature) and the cloud point temperature for each film. An iron-constantin thermocouple was taped to the back of each slide prior to placing it into a heavy-walled glass test tube. The test tube was immersed into a temperature-regulated silicone oil bath.

The objective of the experiment was to determine the temperature where the first faint cloudiness of each film appeared and disappeared as temperature was gradually raised and lowered. Each film was observed using a microscope illuminator. The temperature of the oil bath was raised at 0.2°/min or less until the first faint opalescence was detected in the film. This temperature was recorded. The film was best observed at a low angle of back or forward scattering relative to the incident light. The temperature was gradually increased until a distinct cloudiness in the film was observed. From this point, the cycle was reversed. The temperature was gradually decreased at the same rate until the faintest opalescence just disappeared. This temperature was also recorded.

Although the technique was somewhat subjective, it was found to give reasonably reproducible results. The cycle could be repeated without changing the results by more than a 1-2° statistical error.

(27) M. Bank, J. Leffingwell, and C. Thies, *J. Polym. Sci., Part A*, **2**, 1097 (1972).

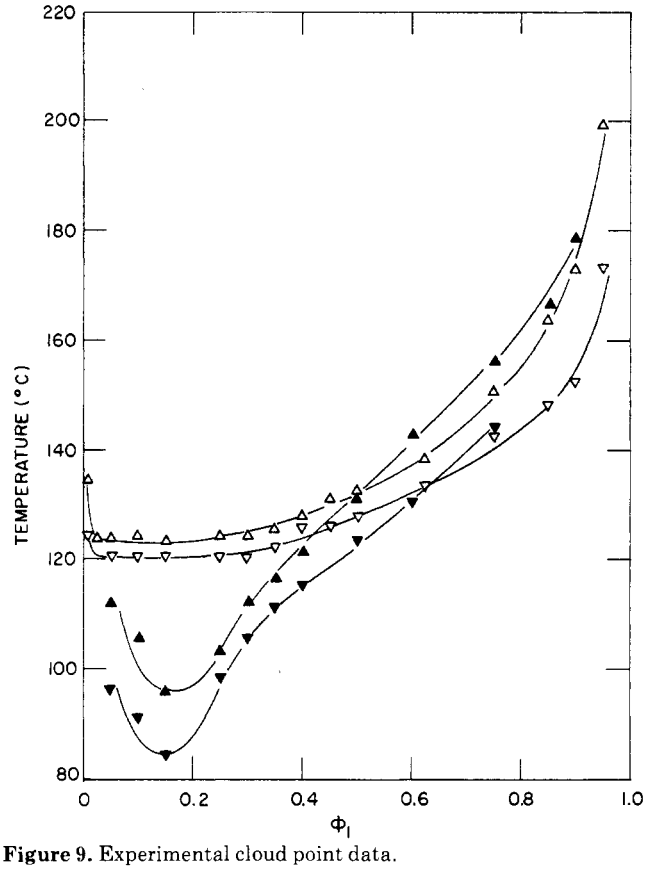

Figure 9. Experimental cloud point data.

Symbol	System
△	Polystyrene-poly(vinylmethylether)—Heating
▽	Polystyrene-poly(vinylmethyl ether)—Cooling
▲	Styrene-acrylonitrile-polycaprolactone—Heating
▼	Styrene-acrylonitrile-polycaprolactone—Cooling

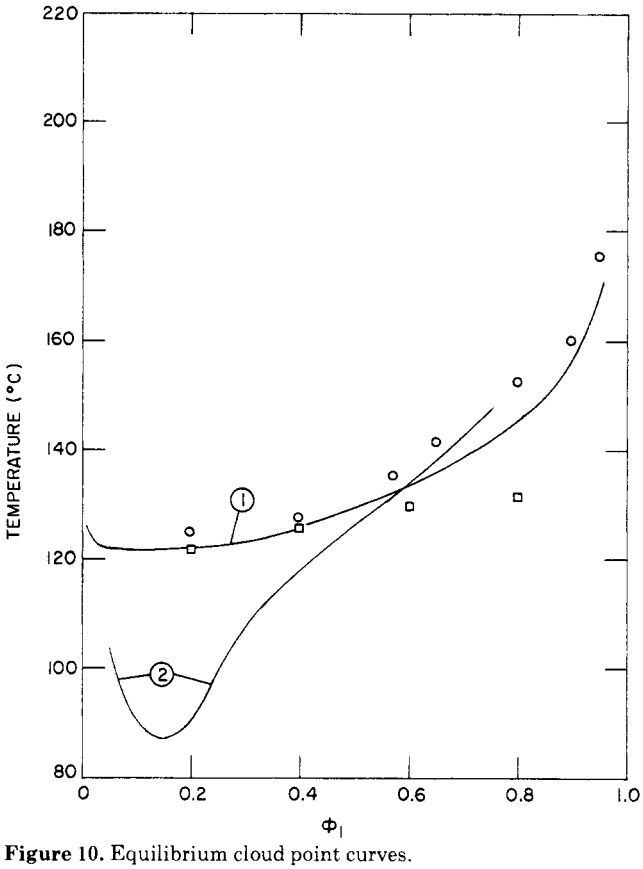

Figure 10. Equilibrium cloud point curves.

Curve	System
1	Polystyrene-poly(vinylmethyl ether)
2	Styrene-acrylonitrile-polycaprolactone
Symbol	
○	Data of Bank, Leffingwell, and Thies,[27] blue tinge
□	Data of Bank, Leffingwell, and Thies,[27] opalescence expolated to zero heating rate

B. Experimental Results. The raw experimental data are plotted for both systems in Figure 9. In each case, the symbol with the triangle pointing up indicates the onset of incipient cloudiness on increasing temperature. The symbol with the triangle pointing downward indicates the point where the last vestiges of cloudiness are observed with decreasing temperature.

The fact that the CPC's measured on increasing and decreasing temperature do not agree can be attributed to several factors. The first is a purely kinetic factor. The heating and cooling rates were finite. An infinitesimally slow temperature excursion is required to allow sufficient time for the diffusion-controlled phase separation process to equilibrate.

The second factor is also a kinetic factor, but it arises from a different source. Except in the vicinity of the critical point, a finite supersaturation is required to cause the nucleation rate to increase to a level sufficient to observe a macroscopic phase transition. This is required because the homogeneous phase is metastable rather than unstable.[23] Indeed, Heady[28] has found that the cloud point for the system C_7F_{14}–C_7H_{14} is insensitive to rates of temperature excursion between 10^{-4} and 10^{-1}°/min. However, in the vicinity of the critical point, the homogeneous system becomes thermodynamically unstable very close to the binodal curve. In this case, spinodal decomposition should lead to phase separation without the necessity of obtaining large supersaturations.[29]

Two factors prevent the precise location of the critical point. The first is that spinodal decomposition occurs at finite rates only after passing beyond the spinodal. The second is that the phase transition point is observable only when sufficient refractive index differences exist to scatter an observable quantity of light. Since both equilibrium phase compositions approach one another at the critical point, it is obvious that temperatures somewhat in excess of the critical point are required to observe the phase transition. This latter factor does not affect the gap width on heating or cooling. Both factors lead to a finite excursion above the lcst.

With these factors in mind, it seems reasonable to attribute the minimum temperature gap to purely kinetic factors. For the PS-PVME system, this gap is approximately 3.5°. It is 5.5° for the SAN-PCL system. In the absence of other data, it seems reasonable to correct the upper CPC by lowering the temperature by half of the gap width measured at the critical point. Also, the lower CPC is corrected by raising it half of the gap width. The remaining gap width at compositions far from the critical composition can be attributed to requiring finite supersaturations in order to attain reasonable nucleation rates. Indeed, electron microscopic evidence (to be reported later) supports the contention that nucleation and growth is the mechanism of phase separation far from the critical point whereas spinodal decomposition occurs for compositions near the critical point.

The final corrected CPC's for these two systems are presented in Figure 10. Also shown are the recently published data of Bank *et al.*[27] on the PS-PVME system. The circle data points correspond to their observations of a faint bluish tinge obtained on heating the samples at a relatively high heating rate (20°/min). They also present data corresponding to the appearance of a distinct opalescence. When these latter data are extrapolated to an infinitesimally slow heating rate, the square data points of Figure 10 are obtained. Both sets of measurements confirm the observations of this work except for the extrapolated data at high polystyrene concentrations. Here the deviations are greater than the normally encountered experimental error for measurements of this type.

These experimental CPC's can be compared to the binodal curves computed using the equation of state thermodynamics. The experimental data show far less sensitivity to temperature than the computed curves. There may be several logical reasons for this qualitative difference. The most important reason may lie in the inaccuracy of Flory's equation of state for the pure components. Recently, it has become obvious that the Flory equation of

(28) R. B. Heady, Ph.D. Thesis, Mass. Inst. Tech., Cambridge, Mass., 1969.

(29) Spinodal decomposition occurs spontaneously whenever the homogenous system is thrust beyond the spinodal. See Cahn[23] for a description of the kinetics of spinodal decomposition.

state predicts too great a variation in the pure component reduced volumes as a function of temperature.[20,25,30] Flory's method of avoiding these difficulties is to measure the equation of state parameters at the temperatures of interest and not to extrapolate too far from these temperatures. In the future, improved equation of state models are needed in order to make quantitative predictions of phase behavior.

A second factor which cannot be neglected is that these polymers are polydisperse. The CPC's of polydisperse systems cannot be compared directly to the monodisperse binodal curves. The CPC of the SAN–PCL system does show a dimple on the right ascending branch. A dimple of this type should be expected near the critical point of a polydisperse polymer pair. Computational techniques have recently been developed so that the effects of polydispersity on the shape of CPC's can be more fully studied.[31] However, calculations of this type have not been performed as part of this study.

Finally, it must be remembered that these polymer systems are not nonpolar. Perhaps, specific interactions are also important. In this situation, the functional dependence of the interaction energy term and perhaps even the combinatorial entropy term may be incorrect.

The most important result is that these data confirm the anticipated lcst behavior predicted by the Flory theory.

Conclusions

A generalized version of Flory's equation of state thermodynamics has been used to explain the phase equilibrium behavior characteristic of polymer–polymer systems. Results of computations made using this theory confirm that lcst behavior should be more common than ucst behavior in polymer–polymer systems. This result is in good qualitative agreement with the experimental observations presented in this study.

The most important equation of state parameter controlling polymer–polymer solubility is the thermal expansion coefficient. Small differences in pure component thermal expansion coefficients are sufficient to lead to an lcst for two high molecular weight polymers. When energy interactions are negligible, two polymers having molecular weights of 200,000 (chain length ~2000) must have thermal expansion coefficients within 4% of one another to exhibit significant mutual solubility.

When the interaction energy parameter assumes small positive values, simultaneous lcst and ucst behavior is possible. For larger positive values of this parameter, the lcst and the ucst merge to yield hourglass-shaped binodal and spinodal curves. The range of X_{12}' values where simultaneous lcst and ucst behavior can occur is small. Hence, this type of phase behavior should be fairly uncommon. When the interaction parameter assumes increasingly negative values, the mutual solubility of the polymer pair increases. The binodal and spinodal curves tend to flatten out showing decreased temperature sensitivity. Negative values of the interaction energy parameter should be anticipated whenever strong hydrogen-bonding or acid–base interactions exist.

The application of increased pressures to two polymers usually causes the lcst (and hence mutual solubility) to increase. However, large differences in pure component thermal pressure coefficients cause the lcst first to decrease and then to increase as the applied pressure is increased.

When two polymers are polydisperse rather than monodisperse, the spinodal curve remains unchanged if the weight-average chain length is substituted into the spinodal equation for the monodisperse chain length. The critical point shifts to either the left or the right ascending branch of the spinodal curve, depending upon the a_1/a_2 ratio. For $a_1/a_2 > 1$, the critical point shifts to higher segment fractions of component 1. For $a_1/a_2 < 1$, it shifts to higher segment fractions of component 2. Determination of the binodal and cloud point curves requires more complex computations. These calculations have not been made, but the qualitative shape of the CPC has been indicated.

Experimental results have confirmed the lcst behavior for two polymer–polymer pairs. The differences in cloud points on increasing and decreasing temperatures have been explained based upon a nucleation barrier for compositions far from the critical composition. The experimental CPC's are less temperature sensitive than binodal curves computed using equation of state thermodynamics. Several reasons for the quantitative difference between theory and observation are suggested.

Acknowledgments. The author thanks the Union Carbide Corp. for permission to publish this work. A special note of thanks is also extended to Mr. E. B. Trzaska and Mr. J. D. Whalen for performing the cloud point and molecular weight determinations, respectively.

(30) B. E. Eichinger and P. J. Flory, *Macromolecules*, 1, 285 (1958).
(31) R. Koningsveld, *Chem. Zvesti*, 26, 263 (1972).